PKCζ regulates cell polarisation and proliferation restriction during mammary acinus formation

Jacqueline Whyte[1,*,‡,§], Laura Thornton[1,‡], Sara McNally[1], Sarah McCarthy[1], Fiona Lanigan[1], William M. Gallagher[1], Torsten Stein[2] and Finian Martin[1,§]

[1]UCD Conway Institute and School of Biomolecular and Biomedical Science, University College Dublin, Belfield, Dublin 4, Ireland
[2]Division of Cancer Sciences and Molecular Pathology, Section of Pathology and Gene Regulation, University of Glasgow, Glasgow, G11 6NT, Scotland, UK

*Present address: Physiology and Medical Physics, Royal College of Surgeons Ireland, 123 St Stephen's Green, Dublin 2, Ireland
‡These authors contributed equally to this work
§Authors for correspondence (jacquelinewhyte@rcsi.ie; finian.martin@ucd.ie)

Accepted 11 June 2010
Journal of Cell Science 123, 3316-3328

doi:10.1242/jcs.065243

Summary

Mammary epithelial cells organize in three dimensions and generate acini when supported on laminin-rich extracellular matrix. Acinus formation begins with the apicobasal polarisation of the outer cells of the assembly and the withdrawal of these cells from the cell cycle. Internal cells then clear out to form a hollow lumen. Here, we show that PKCζ is phosphorylated (at T410) and activated in the early stages of acinus formation in both primary cells and MCF10A cells, and during mammary tree maturation in vivo. Phospho-PKCζ colocalised with tight junction components and bound to the Par polarising complex in developing acini. To further investigate the importance of PKCζ phosphorylation in this context, acinus formation was studied in MCF10A cells overexpressing non-phosphorylatable (T410A) or 'constitutively phosphorylated' (T410E) PKCζ. In both cell types, acinus-associated cell polarisation and lumen clearance were compromised, emphasising the importance of regulated phosphorylation of PKCζ at T410 for successful acinus formation. PKCζ can be activated in a phosphorylation (at T410)-dependent and a phosphorylation-independent manner. Cells overexpressing a complete kinase-deficient PKCζ (K281W) displayed a cell polarising deficit, but also generated large 'multi-acinar' structures with associated early lumenal cell hyperproliferation. Therefore our data shows, for the first time, that two separable PKCζ activities (one phosphorylation-dependent, the other not) are required to support the cell polarisation and proliferation restriction that underpins successful acinus formation. Paralleling these contributions, we found that low levels of PKCζ mRNA expression are associated with more 'poorly differentiated' tumours and a poor outcome in a cohort of 295 breast cancer patients.

Key words: Mammary gland, Epithelial, Cell polarity, PKCζ, Proliferation, Breast cancer

Introduction

Mammary epithelial cells (MECs) form acini when cultured on laminin-rich extracellular matrix (ECM) in vitro. Acini are reminiscent of epithelial cysts seen in the mammary gland in vivo; the constituent cells will establish apicobasal polarity and form a hollow central lumen (Barcellos-Hoff et al., 1989; Blatchford et al., 1995; Blatchford et al., 1999; Weaver et al., 2002). After several rounds of cell division, the monolayer of cells in contact with the ECM establishes apicobasal polarity and these cells withdraw from the cell cycle. Adhesion and tight junction formation precedes the establishment of polarity, and polarisation is thought to precede a suppression of proliferation and the initiation of lumen formation (Debnath et al., 2002; Shin et al., 2006).

It has been proposed that polarisation in an epithelial sheet is initially established following the generation of an active Par signalling complex. The Par complex was first recognised when studies in *Caenorhabditis elegans* identified a family of six *par* genes (partitioning defective) involved in the asymmetric division of the one cell embryo (Kemphues et al., 1988). Central to the Par complex is PKCζ. Several studies have implicated PKCζ as a direct substrate for phosphorylation at threonine 410 (T410) by phosphoinositide-dependent protein kinase 1 (PDK1), which is activated downstream of phosphoinositide 3-kinase (PI3K) and insulin (Chou et al., 1998; Standaert et al., 1997). However, it has also been shown that PKCζ activity can be directly triggered through interactions with the Par complex in a Cdc42-dependent fashion (Plant et al., 2003). Rho-family GTPases, including Cdc42, Rac1 and RhoA, regulate the actin cytoskeleton and cell adhesion (Fukata et al., 2001a; Fukata et al., 2001b) and have been implicated in cell polarisation in several cell types. Cdc42 was shown to bind and activate Par6 and thereby is known to play an important role in Par-directed cell polarisation (Macara, 2004).

Oncogene expression and excessive growth factor drive disrupt mammary cell acinus formation (Debnath and Brugge, 2005; Reginato et al., 2005). Interestingly, expression of activated ErbB2 was found to recruit Par6 and PKCζ from its association with Par3 in the polarising complex. This disrupted cell polarisation induced lumenal cell survival (but not additional cell proliferation), while blocking acinus maturation (Nolan et al., 2008). In other experiments, the interaction between Par6 and PKCζ was found to uncouple ErbB2-induced disruption of polarised epithelial cell organisation from proliferation control (Aranda et al., 2006). A key regulatory role for PKCζ in epithelial cell organisation is also hinted: In MDCK cells, Suzuki and co-workers demonstrated that the overexpression of a dominant negative form of PKCζ (aPKCkn) severely impacted tight junctions and impaired cell polarisation (Suzuki et al., 2001). In addition, Galvez and co-workers found that PKCζ-deficient mice displayed increased Ras-induced lung carcinogenesis, suggesting a role for this kinase as a tumour suppressor (Galvez et al., 2009).

We now show that PKCζ kinase activity is essential for the establishment of cell polarity in primary mouse and MCF10A mammary acini. PKCζ is activated by phosphorylation at T410, forms a complex with activated Cdc42, and complexes with Par3 and Par6 at tight junctions early in primary acinus development. We also show that phospho-PKCζ levels increase dramatically during pubertal development, a period associated with the most significant relative expansion and functional differentiation of the mammary epithelium. We show that acini expressing the T410A (threonine replaced by alanine) PKCζ mutant (that cannot be phosphorylated at T410) are unpolarised and do not clear out their lumena. And, unexpectedly, overexpresssion of the 'kinase-dead' K281W (lysine replaced by tryptophan) PKCζ mutant (which is resistant to activation by any mechanism) induces formation of hyperproliferative, 'multi-acinar' structures; suggesting a tumour suppressor potential for PKCζ. This potential is supported by a screen of 295 human breast tumours from a previously published dataset (van de Vijver et al., 2002), in which we found that low expression of PKCζ mRNA was significantly associated with a poor patient outcome.

Results

Cell polarisation accompanies primary mouse mammary acinus formation

Primary mouse MECs rapidly generate unstructured three-dimensional (3D) cell assemblies when plated on a laminin-rich ECM (Matrigel), in the presence of epidermal growth factor (EGF), insulin and hydrocortisone (Fig. 1A) (Murtagh et al., 2004). After 17 hours in culture, the structures were spherical in shape; by 24 hours, lumen clearance had initiated; and 48–72 hours post-plating, a mature acinus had formed that consisted of a single layer of epithelial cells surrounding a hollow lumen. The parallel establishment of cell polarity was reflected by the tight junction component, ZO-1 (Fig. 1A). ZO-1 localised laterally along the cell–cell junctions during the early stages of acinus formation (4 and 17 hours), moved towards the apical end of the outer ECM-associated cells (24 hours) and, finally, stained as punctate spots at the lateral–apical cell border (where tight junctions localise) in mature acini (48 hours). Normal acinus maturation was disrupted when acini developed in the presence of the JNK activity inhibitor, SP600125 (Fig. 1B) (Murtagh et

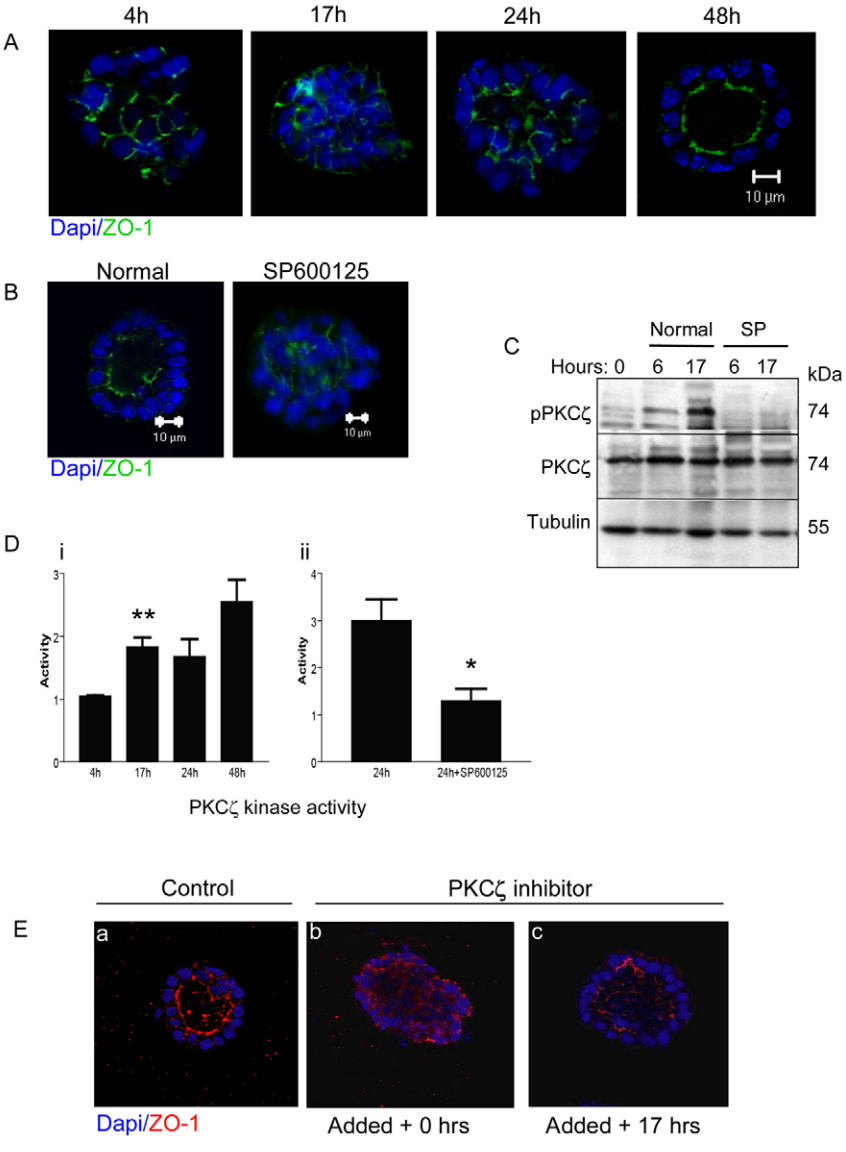

Fig. 1. PKCζ in primary mammary acini. (**A**) Confocal microscopy analysis of primary mouse mammary cells forming acini at 4, 17, 24 and 48 hours. Anti-ZO-1 antibody stains tight junctions green; DAPI stains nuclei blue. Scale bars: 10 μm. (**B**) Acini 48 hours after cell plating in the absence (Normal) or presence of the JNK inhibitor SP600125. (**C**) Western blot analysis of phospho-T410-PKCζ, total PKCζ and tubulin, in whole-cell extracts from acini at 0, 6 and 17 hours after plating, in the absence (Normal) or presence of the JNK inhibitor (SP). (**D**) (Di) PKCζ kinase activity 4, 17, 24 and 48 hours after cell plating onto ECM. Analysis of variance (ANOVA) showed a significant increase in kinase activity with time (P=0.003); value at 17 hours was significantly greater than at 4 hours, **P=0.006, Student's t-test, n=3. (Dii) PKCζ kinase activity when JNK is inhibited (SP); value at 24 hours was significantly less than control, *P=0.03, Student's t-test, n=3. (**E**) Confocal microscopy analysis of acini 48 hours after plating in the absence or presence of the Myr-PKCζ inhibitor, added at time of plating (0 hours) or after 17 hours of culture on ECM; ZO-1 (red), DAPI labels nuclei (blue).

Scaleal., 2004). When JNK was inhibited, characteristic spheroid structures formed, which were filled with unpolarised cells, and apical–punctate ZO-1 localisation failed (Fig. 1B). This study did not examine how JNK supports acinus formation, but rather, JNK inhibition was used as a means of inducing the formation of a dysmorphic acinus in which to examine polarity regulators. As with the expression of some oncogenes (Debnath and Brugge, 2005), JNK inhibition permits sustained EGF signaling and ERK activation with resultant disruption of acinus maturation. Its effects are fully reversed by inhibiting ERK activation (supplementary material Table S1).

PKCζ activity is necessary for acinus formation

We investigated whether the polarity regulator PKCζ plays a role in the polarisation of mammary acini, as has been found in other systems. Like other members of the PKC family, mechanisms of PKCζ activation are complex and appear to be context-dependent. Following phosphorylation of the activation-loop threonine, i.e. T410 in PKCζ, autophosphorylation of the catalytic domain occurs (Keranen et al., 1995; Tsutakawa et al., 1995). This leads to full activation of the enzyme and phosphorylation of substrates. An inhibitory sequence known as the 'pseudosubstrate' domain (PS) is present in the amino terminus of all PKCs including PKCζ (see later), and is thought to confer auto-inhibition by binding to the substrate-binding site and masking one or more phosphorylation site(s) (Gschwendt et al., 1991). Upon lipid binding, a conformational change relieves this auto-inhibition, allowing phosphorylation to occur. PKCζ activity can also be directly triggered through interactions with the Par complex in a Cdc42-dependent fashion (Plant et al., 2003). Therefore, PKCζ can be activated in a phosphorylation (at T410)-dependent and phosphorylation-independent manner.

We examined the phosphorylation status of PKCζ at T410 in developing acini, using an anti-phospho-T410-PKCζ-specific antibody (Etienne-Manneville and Hall, 2001). Robust phosphorylation of PKCζ at T410 occurred very early during acinus development (6 and 17 hours) (Fig. 1C, Normal). This event did not occur in a dysmorphic acinus (Fig. 1C, SP). In parallel, PKCζ kinase activity increased significantly during early acinus maturation (Fig. 1Di), and was significantly lower in a dysmorphic acinus (Fig. 1Dii). Thus, normal acinus formation and associated cell polarisation is paralleled by increases in PKCζ phosphorylation at T410 and kinase activity.

We then tested whether acinus formation and associated cell polarisation is specifically dependent on PKCζ activity. Cell assemblies generated in the presence of a specific myristoylated PKCζ psuedosubstrate inhibitor (Standaert et al., 1999) failed to mature into polarised acini if the inhibitor was added to the cells at the time of plating. They failed to localise ZO-1 to the apical–lateral cell boundary or to achieve lumen clearance (Fig. 1Eb). However, if acini developed for 17 hours before the addition of the inhibitor, no effect on acinus development or polarisation was observed. ZO-1 was correctly localised and lumen clearance occurred (Fig. 1Ec). Thus, in this case, PKCζ activity would seem to be required for the establishment rather than the maintenance of polarity, as has been reported in other systems (Capaldo and Macara, 2007; Margolis and Borg, 2005). Phosphorylation of PKCζ at T410 was not disrupted by this inhibitor in primary mouse acini (supplementary material Fig. S1), or in MCF10A acini (see later).

Phospho-PKCζ, Par3, Par6 and ZO-1 colocalise during acinus formation

It has been shown in other polarising epithelia that PKCζ forms a ternary complex with the PDZ-domain-containing proteins Par3 and Par6 and that this complex becomes localised to areas of tight junction formation (Lin et al., 2000; Suzuki et al., 2001). In mature lumen-cleared primary mammary acini, i.e. by 48 hours, we confirmed that Par3 and ZO-1 colocalised at the tight junction sites at the lateral–apical boundaries of the surviving ECM-associated monolayer of cells (Fig. 2Aa–c). The localisation of phospho-PKCζ paralleled that of ZO-1 (shown at 48 hours) (Fig. 2Ad–f; supplementary material Fig. S1). These also colocalised at cell boundaries *early* in acinus development, suggesting that phospho-PKC colocalises with ZO-1 before reaching the apical membrane and tight junction sites (supplementary material Fig. S1). Analysis of red and green fluorescence intensities at the punctate apical–lateral border sites revealed that the two fluorescence outputs (anti-ZO-1 and anti-phospho-PKCζ) coincided in mature acini (Fig. 2Bg,h).

In MDCK epithelial cells, it has been shown that tight junction formation requires that PKCζ complexes with Par3 and Par6 in a Cdc42-dependent manner, with the resultant activation of PKCζ (Joberty et al., 2000; Qiu et al., 2000). We found that as primary mouse mammary acini formed (at 17 and 24 hours), PKCζ immunoprecipitated in a complex with Par3 (Fig. 2B,C; supplementary material Fig. S2). In addition, Par3 and PKCζ formed a complex with Par6 (Fig. 2D). However, in dysmorphic acini, PKCζ was not detected in a complex with either Par3 or Par6 (Fig. 2B–D). This suggests that PKCζ only forms a stable complex with Par3 and Par6 as the cells become polarised. Interestingly, we could demonstrate that the PKCζ complexed with Par3 was phosphorylated on T410 (Fig. 2C). We detected two bands using anti-Par3 antibodies, with the band at 100 kDa being the most prominent (supplementary material Fig. S2). Thus, the PKCζ kinase activity required for acinus cell polarisation is associated with PDZ-domain-containing protein complexes and localizes to tight junction sites.

Activation of the GTPase Cdc42 regulates the organisation of the actin cytoskeleton and is required to establish asymmetry during epithelial morphogenesis, asymmetric cell division and directed cell migration. Also, Cdc42 was shown to interact with Par complex proteins to drive cell polarisation in rat astrocytes (Etienne-Manneville and Hall, 2001; Gotta et al., 2001; Macara, 2004). We used GST-tagged PBD (p21-binding domain) of Pak1 (p21 activated kinase 1) to specifically pull-down active (GTP-bound) Cdc42 from primary acini. We found active Cdc42 early during primary mouse mammary acinus development, at 6 and 17 hours (Fig. 2E); and reduced levels in dysmorphic acini (SP). In addition, we detected phospho-T410-PKCζ in a complex with the active Cdc42 (Fig. 2F). We conclude that a complex containing phospho-T410-PKCζ and active Cdc42 necessarily forms early during acinus development.

PKCζ activity is required for polarisation in MCF10A acini

MCF10A cells are an immortalised but non-transformed human MEC line. We used MCF10A cells to validate our findings from the primary cell acini and to facilitate genetic manipulation. Similarly to primary cells, MCF10A formed acini on the basement membrane (Debnath et al., 2003). Fully cleared and polarised MCF10A acini were observed 14–16 days after plating on ECM (Fig. 3A). At day 4 (D4), assemblies were a spheroid of cells that

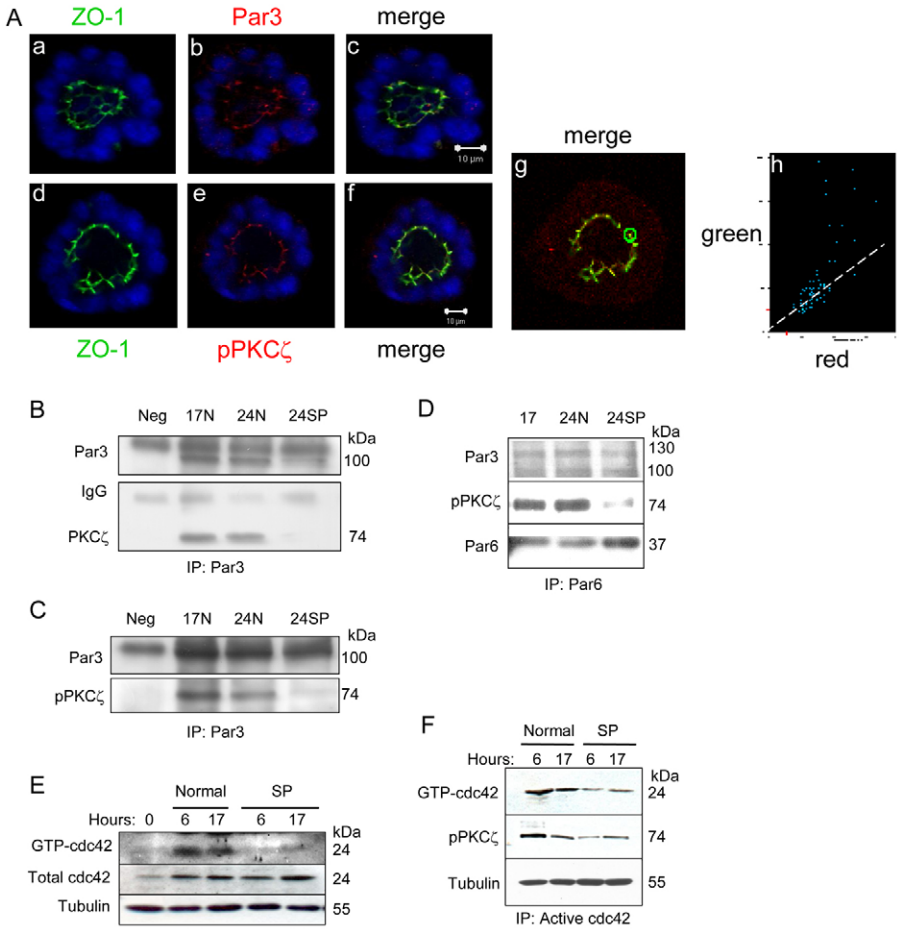

Fig. 2. Phospho-PKCζ interacts with Par proteins and active Cdc42 in developing primary acini. (**A**) Confocal microscopy analysis of normal mature acini (48 hours). ZO-1 (green) and Par3 (red) colocalise at apical puncta (merge) (Aa–c). ZO-1 (green) and phospho-PKCζ (red) also colocalise at apical puncta (merge) (Ad–f). A punctate region of co-expression of ZO-1 and phospho-PKCζ (green/red) is highlighted by the green circle (Ag). Expression intensities of both red and green pixels are plotted (Ah). Distribution of pixels confirms colocalisation; DAPI (blue). Scale bars: 10 µm. (**B**) Extracts prepared from acini 17 and 24 hours after plating (and with SP600125 to inhibit JNK) were immunoprecipitated with an anti-Par3 antibody. The immunoprecipitate was analysed by western blot analysis using anti-Par3 and anti-PKCζ. We see two bands with antibodies to Par3 (see also Fig. 2C; supplementary material Fig. S2). (**C**) As B, except that the immunoprecipitate was analysed by western blot analysis using anti-phospho-PKCζ. (**D**) As C, except that extracts were immunoprecipitated with anti-Par6 antibody. The immunoprecipitate was analysed using anti-Par6, anti-Par3 and anti-phospho-PKCζ antibodies. (**E**) Active Cdc42 was pulled down (see Materials and Methods) from acinar extracts at 0, 6 and 17 hours after plating of cells (and with SP600125 to inhibit JNK). (**F**) Western blot analysis of pulled-down active/GTP-Cdc42 shows that phospho-PKCζ is detectable in a complex with GTP-Cdc42 at 6 and 17 hours in normal developing acini, and that the amount of this complex is diminished in dysmorphic acini (SP).

were mostly unpolarised. By day 8 (D8), two populations of cells were clearly evident: An ordered, polarised outer layer of cells could be clearly distinguished from those remaining in the lumen (Fig. 3A). Anti-Ki67 immunostaining showed that the D8 cells had mostly ceased proliferating (Fig. 3Ba), β-catenin had become distributed to the basolateral membrane (Fig. 3Bb), and Gm130 (a Golgi marker) was concentrated apically (Fig. 3Bc). Cleaved caspase 3 staining was confined to the lumenal cells, reflecting their loss, at least in part, by apoptosis (Fig. 3Bd).

Fig. 3Ca–c again shows that by D4, spheroids of cells were unpolarised, but that by D8, two distinct populations of cells could be seen (Fig. 3Cd–f). Treatment with SP600125 to inhibit JNK activity resulted in no cell polarisation (as reflected by β-catenin staining), no separation of cells into two populations, and no evidence of the initiation of lumen clearance (Fig. 3Cg–i). To investigate whether active PKCζ is required for MCF10A cell polarisation, developing acini were treated with the myristoylated PKCζ pseudosubstrate peptide inhibitor. We saw no establishment of cell polarisation (β-catenin was no longer basolateral) and no evidence of lumen clearance (Fig. 3Cj–l). Failure to establish cell polarity was also confirmed using staining for the apical marker Gm130 after inhibition of PKCζ and JNK (see later). Thus, as with the primary system, JNK supports MCF10A acinus assembly, and PKCζ activity is required for cell polarisation and eventual acinus maturation.

We also observed a low level of phosphorylation of PKCζ at T410 and high levels of phospho-ERK in the JNK-inhibited MCF10A spheres (Fig. 3D); again also seen previously in the primary system (McArdle, E., unpublished observation). Although T410 of PKCζ is available for phosphorylation, the kinase is inactive after pseudosubstrate treatment (Standaert et al., 1999).

Overexpression of a PKCζ mutant, resistant to phosphorylation at T410, blocks cell polarisation during acinus formation

To specifically investigate the importance of phosphorylation at T410 of PKCζ, lentiviruses that transduce ‘phosphorylation-resistant’ PKCζ (T410A PKCζ; threonine to alanine mutation), and a constitutively ‘phosphorylated’ mimic (T410E PKCζ; threonine to glutamic acid mutation) were generated (Fig. 4A) (Chou et al., 1998). We obtained ~100% infection of MCF10A monolayers and GFP intensity appeared homogenous (Fig. 4B). Empty vector (EV)- and wild-type (WT)-PKCζ-infected MCF10A cells appeared normal in monolayer culture and successfully matured into acini over 2 weeks, similarly to non-infected cells (Fig. 4Ba–h). Cells overexpressing T410A PKCζ appeared similar to controls, but those expressing T410E PKCζ (the form designed to mimic PKCζ with phosphorylated T410) were larger, displayed many extended protrusions, and some cells were markedly rounded up (Fig. 4Bm–p). These cells appeared to have lost their epithelial phenotype.

After 8 days of normal acinus development, the outer MCF10A cells in contact with ECM were polarised, as reflected by the apical localisation of Gm130 (Fig. 3Be, Fig. 5Aa) and (as observed previously) by the basolateral distribution of β-catenin (Fig. 3Bb,Ce). Acini failed to establish cell polarity and mis-localised

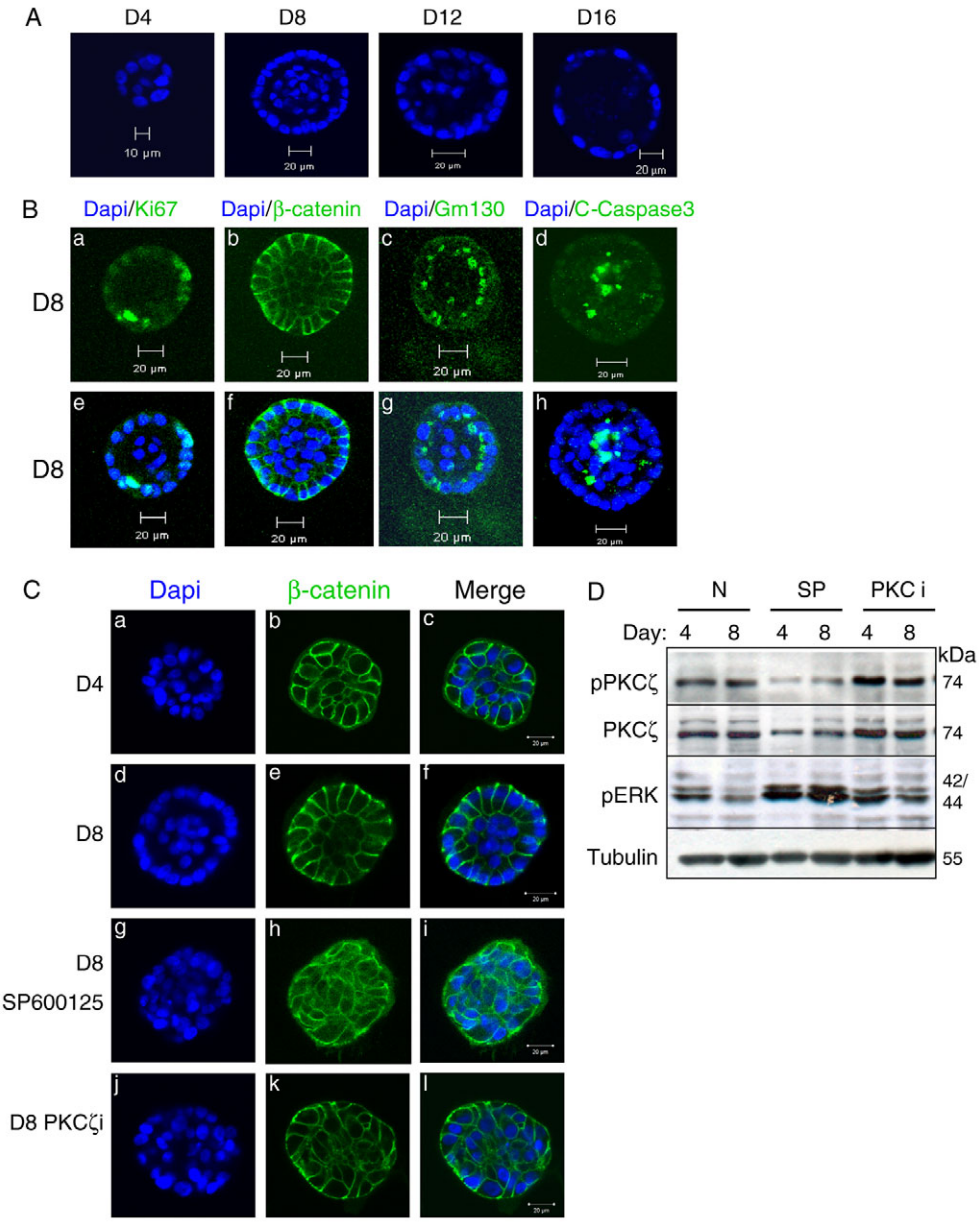

Fig. 3. MCF10A cells require JNK and active PKCζ to form acini. (**A**) Confocal microscopy analysis of MCF10A acini (cultured on ECM) from days 4-16; DAPI (blue). (**B**) MCF10A acini were cultured for 8 days and immunostained with (Ba) anti-Ki67, (Bb) anti-β-catenin, (Bc) anti-Gm130 and (Bd) anti-cleaved caspase 3 antibodies (DAPI blue; merge shown). Scale bars: 20 μM. (**C**) At D4, β-catenin (green) localises laterally at cell membranes in an unpolarised manner (Ca–c). By D8, β-catenin redistributes to the basolateral membrane (Cd–f). When JNK activity is inhibited (SP600125) (Cg–i), or when PKCζ is inhibited (PKCζi) (Cj–l), β-catenin does not localise to the basolateral membranes and there is no lumen clearance. Scale bars: 20 μm. (**D**) Western blot analysis of MCF10A extracts from D4 and D8 of acinus development in presence and absence (N) of JNK inhibitor (SP) and PKCζ inhibitor (PKCζi), analysed for phospho-PKCζ, total PKCζ, phospho-ERK and tubulin.

Gm130 upon JNK blockade (using SP) (Fig. 5Ab) and also in the presence of the myristolated PKCζ pseudosubstrate inhibitor (PKCζ i) (Fig. 5Ac). Virally transduced cells overexpressing EV PKCζ and WT PKCζ formed normal polarised spheres (Fig. 5Ba–d), although the latter took ~2 days longer to clear out their lumena. By contrast, the outer ECM-associated cells in acini overexpressing the non-phosphorylatable T410A PKCζ mutant did not polarise (as reflected by the non-apical localisation of Gm130) (Fig. 5Be), further confirming that phosphorylation of PKCζ at T410 is required for cell polarisation during acinus formation. Interestingly, cells overexpressing T410E PKCζ (constitutively 'phosphorylated' mimic) did not polarise either (Fig. 5Bg). Expression of either of these mutant forms of PKCζ also caused mis-localisation of β-catenin and Scribble from basolateral membranes (not shown). FLAG tags were detected in extracts of acini at the correct molecular weight by western blotting, and GFP levels were homogenous, as shown by both immunofluorescence and western blot analysis (Fig. 4B, Fig. 5C).

Overexpression of kinase-dead PKCζ induces the formation of multi-acinar structures

Mutation of lysine 281, in the ATP-binding region of PKCζ, to tryptophan (PKCζ K281W) generates a 'kinase-dead' PKCζ (Fig. 6A) (Cenni et al., 2002). Overexpresssion of PKCζ K281W had a different and more severe effect on MCF10A acinus behaviour than overexpression of PKCζ with mutated T410. In monolayer culture, cells appeared phenotypically normal; however, populations of cells expressing PKCζ K281W appeared to be more dense (Fig. 6Be), suggesting a higher proliferation rate. To further investigate the hyperproliferation, we examined cell viability and proliferation rates via MTT assay. We observed that cells expressing PKCζ K281W grow significantly faster in monolayer culture than do cells overexpressing EV PKCζ (Fig. 6C) ($P<0.0085$).

In 3D culture, the cells overexpressing PKCζ K281W formed large multi-acinar structures, similar to those observed when overexpresssed ErBb2 is constitutively activated (Muthuswamy et al., 2001) (Fig. 6Bh, black arrows, and Fig. 7Ac,d). The numbers

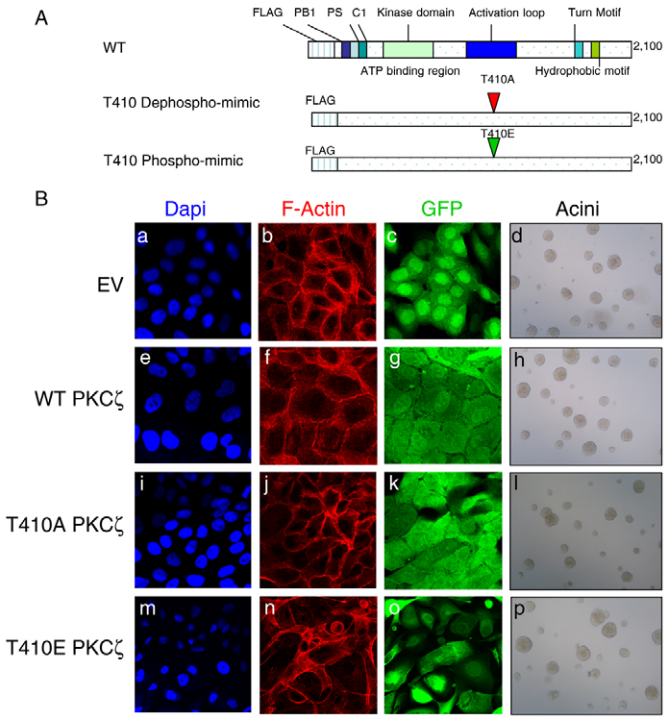

Fig. 4. Overexpression of T410 mutant PKCζ in MCF10A cells. (**A**) Scheme adapted from Hirai and Chida (Hirai and Chida, 2003). Domains: PB1 in N terminus, PS (pseudosubstrate), C1 domain, kinase domain. The ATP-binding region, activation loop, hydrophobic domain and a turn motif are shown. T410 in the activation loop undergoes phosphorylation leading to kinase activation in some instances. (**B**) Confocal microscopy analysis of lentivirus-transduced MCF10A monolayers overexpressing EV PKCζ (pWPI) (Ba–d), WT PKCζ (Be–g), T410A PKCζ (Bi–k) and T410E PKCζ (Bm–o). DAPI (blue), actin (red) and GFP (green). Phase-contrast microscopy images (on D10) of mutant-overexpressing cells cultured to form 3D acini are shown in Bd,h,l,p (10× magnification).

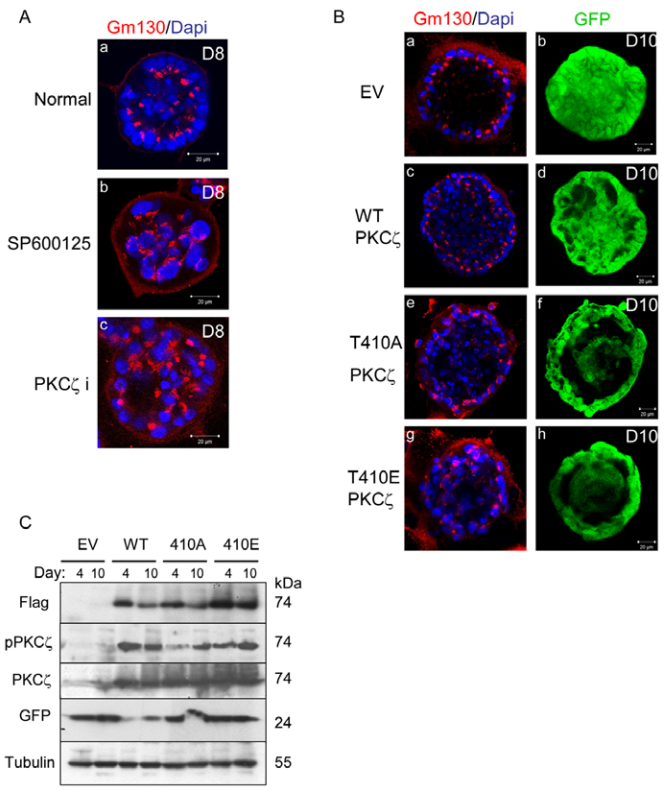

Fig. 5. Overexpression of phospho-T410-resistant PKCζ mutant disrupts polarisation. (**A**) Confocal microscopy analysis of acini on D8: Gm130 (red) localises apically to Golgi membranes in ECM-associated cells, reflecting fully polarised MCF10A cells. Lumen clearance is also advanced (Normal, Aa). In dysmorphic JNK-inhibited (SP600125, Ab) or PKCζ-inhibited acini (PKCζ i, Ac), there are no distinct outer or lumenal cell populations. Gm130, although punctuate, is randomly distributed and there is no lumen clearance; DAPI (blue). Scale bars: 20 µm. (**B**) Control virus transduced cells overexpressing EV PKCζ localise Gm130 apically in a polarised manner and form lumen-cleared mature acini at D10 (Ba,b). ECM-associated WT PKCζ-overexpressing cells distribute Gm130 apically (Bc,d). Cells overexpressing T410A PKCζ (Be,f) and T410E PKCζ (Bg,h) do not distribute Gm130 apically; cells in contact with ECM appear loosely adhered and acini do not clear out their lumena; (GFP, green). Scale bars: 20 µm. (**C**) Western blot analysis of D4 and D10 acini showing FLAG, phospho-PKCζ, PKCζ, tubulin and GFP expression, confirming overexpression of EV, WT, T410A or T410E versions of PKCζ by lentiviral infection of MCF10A cells.

of such structures per field was significantly greater than those formed with either T410 mutant, and it was minimal after infection with EV or WT PKCζ (Fig. 7B). After the initial rounds of cell growth during early acinus maturation, a crucial restriction of cell proliferation occurs (Petersen et al., 1992; Sequeira et al., 2007). Triggered activation of ErbB2 in acini lead to re-initiation of proliferation, filling of their lumenal space and the formation of multi-acinar structures (Muthuswamy et al., 2001). In our multi-acinar structures, we observed strikingly high levels of cell proliferation early during acinus formation, as reflected by high levels of Ki67 staining at D4 but not at D8 (not shown), compared to control acini, which were growth arrested (Fig. 7Cb,e). This was paralleled by increased levels of phospho-p21, phospho-EGFR and phospho-ERK at D4 relative to EV PKCζ (Fig. 7E; supplementary material Fig. S4). These changes could be considered pro-proliferative.

At day ten (D10), the outer ECM-associated cells of the PKCζ K281W multi-acinar spheres showed some evidence of polarisation compared with the phosphorylation mutants (compare Fig. 5Be and Fig. 7Ac). However, no signs of lumen cell clearance were seen in the D10 multi-acinar spheres (in normal acini, lumen clearance would be well advanced by D10) (compare Fig. 7Aa,c). In the multi-acinar spheres, cleaved caspase 3 staining was low-to-normal (Fig. 7De). Thus, complete blockade of PKCζ kinase activity in this way led to high levels of cell proliferation at an early stage of acinus development, with the resulting formation of multi-acinar structures. Interestingly, it resulted in a different phenotype to that seen when phosphorylation of PKCζ at T410 was disrupted. Taken together, these observations suggest that PKCζ activation by phosphorylation at T410 is crucial for polarisation, but that total blockade of PKCζ kinase activity can induce events associated with early stages of breast cancer progression (loss of polarised epithelial cell organisation, hyperproliferation and lumenal filling).

PKCζ in the mouse mammary gland in vivo

We investigated the status of PKCζ phosphorylation in mouse mammary glands at different stages of development. During puberty, the mammary gland develops from a rudimentary tree to

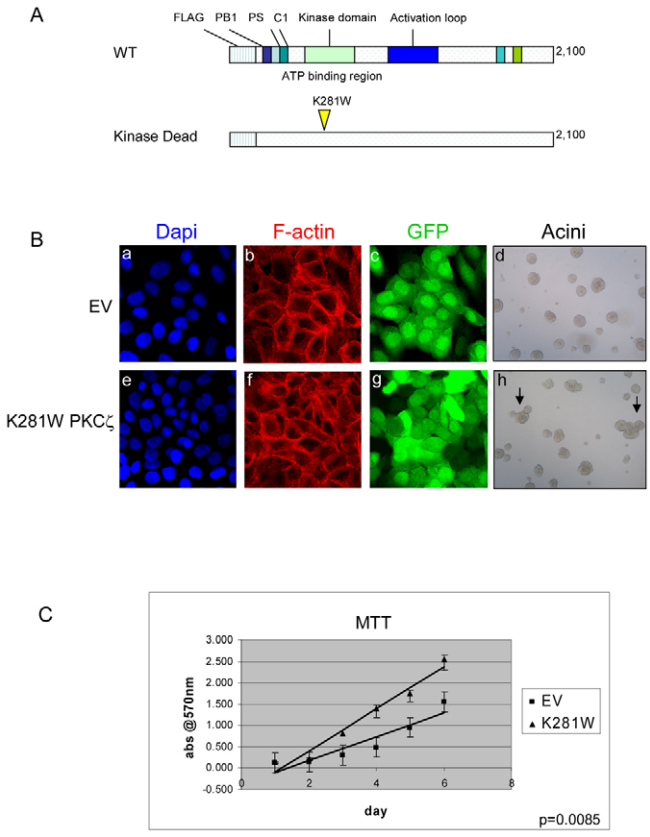

Fig. 6. Overexpression of kinase-dead PKCζ induces hyperproliferation. (**A**) See Fig. 4A. In the ATP-binding region, lysine 281 is crucial for PKCζ kinase activity. (**B**) Confocal microscopy analysis of lentivirus-transduced MCF10A monolayers overexpressing EV PKCζ (Ba–c) and K281W PKCζ (Be–g); actin (red), DAPI (blue), GFP (green). Cells overexpressing EV PKCζ and K281W PKCζ were used to form 3D acini and imaged by phase contrast (Bd,h) (D10). Arrows point to multi-acinar structures in the cells overexpressing K281W PKCζ (10× magnification). (**C**) MTT assay to measure the number of viable cells over 6 days of culture revealed that the cells overexpressing K281W PKCζ proliferated more rapidly than do EV PKCζ-infected cells (P=0.0085, Student's t-test).

a branched epithelial network of ducts, filling the fat-pad. This supports alveolar development during pregnancy and subsequent milk production at lactation. Western blot analysis showed that an increase in phospho-T410-PKCζ levels accompanied epithelisation of the glands at puberty (Fig. 8A). This puberty-associated increase in PKCζ phosphorylation paralleled the expansion of the epithelial content of the glands, as reflected by the increased levels of tight junction (ZO-1) and adherens junction proteins (E-cadherin) at 6.5 weeks (Fig. 8A). Phosphorylation of PKCζ at 6.5 weeks also correlates with high levels of active Cdc42, and these had already risen by 4 weeks (not shown). This phosphorylation (activation) of PKCζ would seem to be a 'specific' event and not a reflection of a 'general' activation of signalling pathways associated with pubertal ductal morphogenesis: there was no increment in the levels of phospho-AKT and phospho-ERK between 4 (pre-pubertal) and 6.5 weeks (pubertal). Confocal microscopy analysis of a transverse section through a duct at puberty (Fig. 8B) showed strong apical phospho-T410-PKCζ staining with colocalisation to ZO-1 at apical punctae (most probably tight junctions). This suggests that in the developing mammary epithelial tree, signalling through phospho-T410-PKCζ might contribute to the establishment of the polarized epithelial sheet that lines the duct in the same way as in acinus development. Of interest is the fact that apical expression of phospho-T410-PKCζ is detectable in large ducts in the pubertal gland, but not in equivalent 'more mature' ducts in the early pregnant gland (however, apical staining of epithelial cells in growing alveoli is seen; see Fig. 8D).

We report a dramatic increase in PKCζ and phospho-T410-PKCζ levels from late pregnancy to early in lactation, with phospho-T410-PKCζ levels then markedly reduced 2 days after the commencement of involution (Fig. 8C). Phospho-T410-PKCζ levels again paralleled increased levels of tight junction (ZO-1) and adherens junction (E-cadherin and β-catenin) proteins, which might reflect the 'functionality' of the epithelial apical barrier in the alveoli in lactation. Interestingly, phospho-T410-PKCζ levels fall in early involution, as the epithelial sheets deteriorate functionally. Thus, PKCζ activation (via T410 phosphorylation) peaks early in lactation, a time when tight junctions are secure, their 'barrier function' established, and the secretary machinery functional (Nguyen and Neville, 1998). From early pregnancy, and increasing in its intensity through pregnancy to early lactation, phospho-T410-PKCζ staining in the mammary gland was associated predominantly with the apical side of the alveolar epithelial cells, becoming more membranous as pregnancy proceeded to early lactation (Fig. 8D). It was to a degree punctate; the staining was lost in early involution (Fig. 8D) and was more concentrated to the apical membrane than total PKCζ staining (which extended more through the cytoplasm; supplementary material Fig. S5); but neither colocalized with ZO-1. Perhaps phospho-T410-PKCζ contributes differently in the mature, differentiated alveolar epithelial cell, we would suggest that it contributes to the secretary machinery.

Low PKCζ expression is associated with shorter patient survival and poorly differentiated tumour grade in human breast cancer

As breast cancer progresses, tumour cell masses become less organised. These cellular changes are often accompanied by altered cell adhesions, a failure of cell polarisation, and increased rates of cell proliferation (Aranda et al., 2008; Baranwal and Alahari, 2009; Kass et al., 2007). Because of the profile of the epithelial cells in which PKCζ activity was disturbed, we investigated the correlation of levels of tumour PKCζ (mRNA) with the outcome of disease in the 'van de Vijver' cohort of 295 patients with breast cancer. All patients had stage I or II breast cancer and were younger than 53 years old, and full clinical information had been gathered. Expression microarray analysis for transcripts was carried out on the primary tumour material (van de Vijver et al., 2002). Two trends were identified by Kaplan–Meier analyses: both low and high levels of PKCζ expression correlated with poor outcome (shorter time to overall survival), with low expression levels being the most significantly associated with a poorer outcome (P=0.041, this P value represents the comparison of low expressers to the group of medium expressers) (Fig. 9A). We also examined the association between PKCζ transcript levels and poorly differentiated tumours, and found that in poorly differentiated tumours, low PKCζ mRNA levels tended to correlate with a poorer outcome (Fig. 9B, P=0.056). Collectively, these analyses support the hypothesis that low levels of PKCζ, which would correlate with low kinase activity, will potentially cause polarity defects, undermine cell proliferation restriction, and disrupt cell organisation

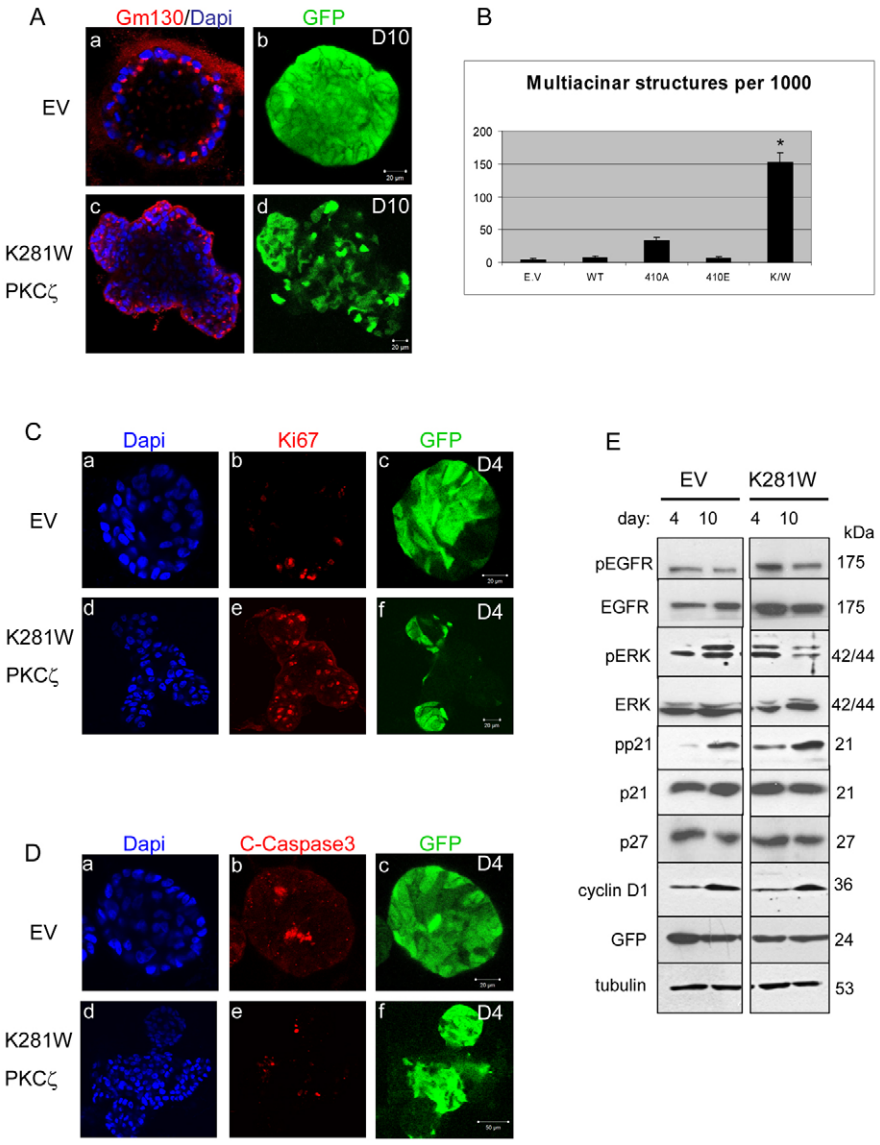

Fig. 7. Overexpression of kinase-dead PKCζ induces the formation of multi-acinar structures. (**A**) EV PKCζ-expressing acini organise normally, clear out their central lumens and polarise/localise Gm130 to the apical region of mature acini (Aa,b). ells overexpressing K281W PKCζ do not organise normally in 3D, do not clear out their central lumens and do not localise Gm130 in a polarised manner (Ac,d); DAPI (blue). Scale bars: 20 µM. (**B**) Graph quantitates the number of multi-acinar structures formed per 1000 cells plated (P=0.003). Number of multi-acinar structures is shown on the y-axis. (**C**) At D4, ki67 (red) levels in K281W PKCζ-overexpressing acini (Cd–f) were significantly higher than control EV PKCζ-expressing acini (Ca–c). Scale bars: 20 µm. (**D**) Cleaved caspase 3 (red) levels in cells overexpressing EV PKCζ and K281W PKCζ were similar at D4; DAPI (blue). Scale bars: 20 µM (Da–c) or 50 µM (Dd–f). (**E**) Western blot analysis at D4 and D10 of development of acini overexpressing EV PKCζ or K281W PKCζ. Phospho-EGFR, phospho-ERK and phospho-p21 levels were higher in cells expressing K281W PKCζ at D4 of acinus development than in EV PKCζ-expressing controls. Total protein levels and p27 levels remained the same. Tubulin and GFP were used as loading controls.

in 3D, thus promoting tumour progression and leading to a poor outcome for patients.

Discussion

The establishment of epithelial cell polarity and cellular adhesions represses pathways for proliferation and promotes those for differentiation, and their loss is commonly associated with loss of tissue integrity in human cancers (Aranda et al., 2008; Brembeck et al., 2006; Hirohashi and Kanai, 2003). Studies in *Drosophila* suggest a relationship between loss of cell polarity and loss of proliferation control (for a review, see Wodarz, 2000). Disruption of polarity complex proteins (such as Scribble) results in uncontrolled proliferation (Zhan et al., 2008), and the restoration of polarity in transformed MECs was found to re-establish growth suppression in 3D systems (Weaver et al., 1997). The establishment of epithelial cell polarity has been shown to be driven by the activities of a Cdc42-regulated complex that contains Par6, Par3 and PKCζ in a range of model systems (including MDCK cells and *C. elegans*) (Joberty et al., 2000; Kemphues, 2000; Kemphues et al., 1988; Lin et al., 2000; Macara, 2004; Qiu et al., 2000). Investigations reveal that the Par complex is restricted to the apical–basal border of polarised epithelia and promotes asymmetry within cells (Bilder et al., 2003; Goldstein and Macara, 2007; Wodarz and Nathke, 2007).

Here, we report a role for PKCζ in establishing the cell polarisation and proliferation restriction necessary for mammary epithelial acinus formation (by both primary mouse and human MCF10A cells). We show the following six results for the first time: (1) Increasing levels of PKCζ kinase activity and phosphorylation of PKCζ at T410 parallels acinus maturation. (2) PKCζ complexes with Par6 and Par3 and with active Cdc42 early in developing primary acini, and phospho-PKCζ and Par3 colocalise with ZO-1 at apical tight junction sites as the acini mature. (3) Inhibition of PKCζ activity (i) by JNK inhibition, (ii) using a pseudopeptide PKCζ-specific inhibitor, and (iii) by overexpression of a non-phosphorylatable PKCζ mutant (PKCζ T410A) is sufficient to inhibit the cell polarisation necessary for acinus formation. (4) In vivo, a significant increase in phospho-T410-PKCζ levels accompanies mouse mammary gland epithelisation at puberty (ductal morphogenesis); and a dramatic increase in phospho-T410-PKCζ levels occurs early in lactation, a time when tight junctions have just closed securely, their ‘barrier

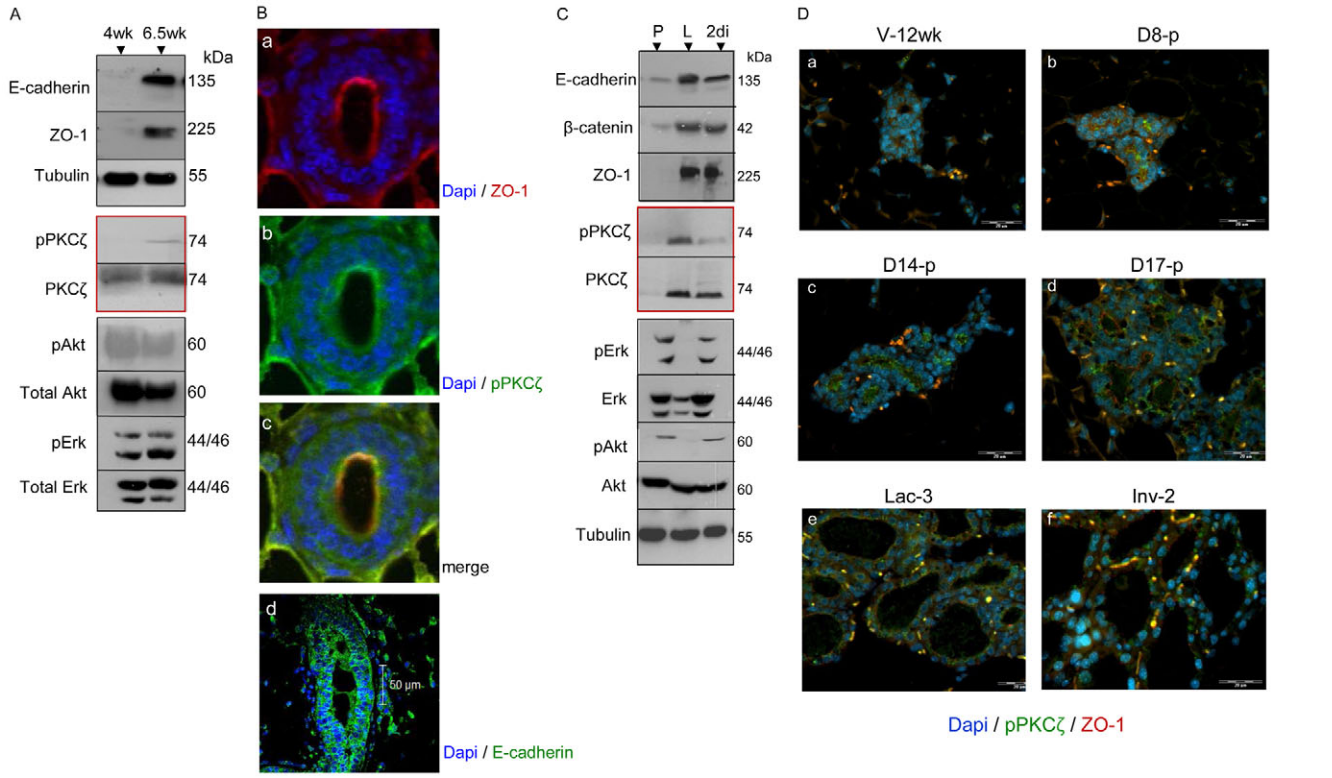

Fig. 8. PKCζ expression in whole mammary glands. (**A**) Western blot analysis of protein extracts from whole mammary glands. In contrast to phospho-ERK and phospho-AKT (whose levels remain the same), adhesion protein induction (E-cadherin and ZO-1) parallels PKCζ phosphorylation at T410 in 4 (pre-pubertal) and 6.5 (pubertal) weeks. Tubulin was loading control. (**B**) Confocal microscopy analysis of a transverse section through a duct at puberty showing phospho-PKCζ staining (green) colocalising with ZO-1 (red) at apical puncta (see merge). E-cadherin shows basolateral localization as a control (Bd). DAPI labels nuclei blue. Scale bar: 50 µM. (**C**) Western blot analysis of protein extracts from whole mammary glands: pregnant (15–16 days) (P), lactating (L) and 2 days post-involution (2di). We report an induction of phospho-PKCζ levels during lactation. Concomitantly, E-cadherin, β-catenin and ZO-1 expression is induced and this pattern is reversed after lactation at involution. By contrast, phospho-ERK and phospho-AKT levels reduced during lactation and increased at involution. Tubulin was loading control. (**D**) Confocal microscopy analysis of in vivo mammary glands from virgin (V-12wk), early pregnancy (D8-p), pregnant (D14-p, D17-p), lactating (Lac-3) and 2 days post-involution (Inv-2), showing phospho-PKCζ staining in the epithelial cells lining the ducts (green). Levels increase at pregnancy and are apically localized and somewhat punctate (Db–d). Little staining is observed at involution (Df). DAPI labels nuclei blue. ZO-1 (red) does not colocalise. Scale bars: 20 µM.

function' has become optimized and secretion established. (5) Expression of kinase-dead PKCζ (PKCζ K281W), which blocks PKCζ activation by any means, leads to incomplete polarisation, but also to high early proliferation and resultant formation of large multi-acinar structures. (6) Low PKCζ transcript expression levels in primary human breast tumours are associated with a poor patient outcome; and in poorly differentiated tumours, low expression levels of PKCζ gives the worst outcome, suggesting that PKCζ protects from deleterious aspects of breast tumour progression.

When JNK activity is inhibited with SP600125, 'dysmorphic' cell assemblies form, cell polarisation and lumen clearance fail, and acinus maturation is blocked. These disorganised spheroids are deficient in tight junction component proteins (Murtagh et al., 2004). If JNK activity is reduced using a peptide inhibitor (JNK inhibitor III, Calbiochem) or using shRNA techniques, a similar effect is observed (McArdle, E. and Whyte, J. unpublished observations; supplementary material Table S1). Using JNK inhibition as a tool to block acinus maturation, we find in parallel: a reduction in PKCζ kinase activity, a failure of PKCζ phosphorylation on T410 (as early as 4 hours after cell plating), loss of association of phospho-PKCζ with Par3, Par6 and Cdc42, and a loss of colocalisation of phospho-PKCζ with ZO-1 at apical tight junction sites. Crucially, cell polarisation and subsequent acinus maturation were paralleled by phosphorylation of PKCζ at T410, its retention in the polarising complex, and its expected selective distribution to tight junctions (as marked by ZO-1). In addition, manoeuvres that block acinus maturation block PKCζ phosphorylation, its complexing with Par proteins and localisation to tight junctions. So, is phosphorylation of PKCζ at T410 necessary for cell polarisation and subsequent acinus maturation? In the MCF10A model, as in the primary cells, inhibition of PKCζ with the pseudopeptide inhibitor inhibited cell polarisation, and polarisation (sub-serving acinus formation) in the MCF10A cells was associated with phosphorylation of PKCζ at T410. Furthermore, the outer layer of cells (those in contact with the ECM) in MCF10A acini overexpressing the non-phosphorylatable T410A PKCζ mutant did not polarise, displayed a distinct 'sphere-within-a-sphere' phenotype (Fig. 5Bf) and did not clear their lumena. This strongly suggests that phosphorylation of PKCζ at T410 is required for cell polarisation during acinus formation. Interestingly, cells overexpressing the T410E PKCζ (constitutively 'phosphorylated' mimic) mutant did not polarise when seeded to form acini. This suggests that, although required, phosphorylation of PKCζ must be properly regulated to drive cell polarisation in early acinus development.

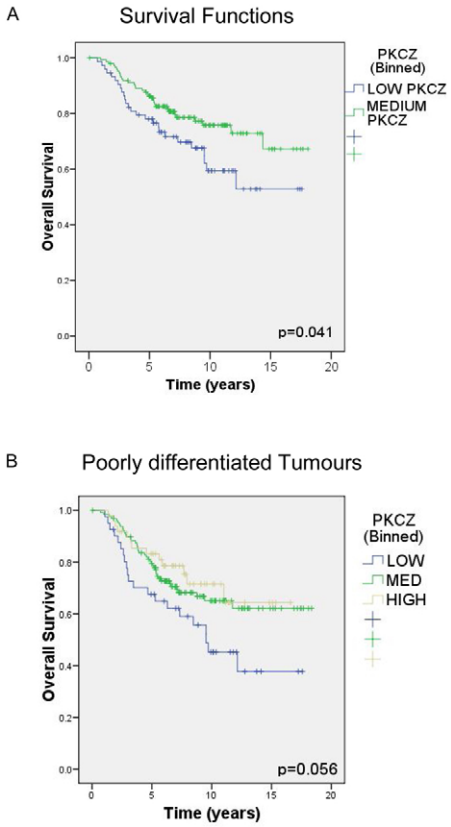

Fig. 9. Low levels of PKCζ mRNA transcripts in human breast cancer patients is associated with a poor outcome. (**A**) Kaplan–Meier analyses examining patient survival and PKCζ expression levels (van de Vijver et al., 2002). Blue indicates low PKCζ expression level and green medium. A low level of PKCζ expression is significantly associated with a poor outcome; *P*=0.041, Log rank (Mantel–Cox) test. (**B**) In poorly differentiated tumours, Kaplan–Meier analyses revealed that low PKCζ expression level is associated with a poorer outcome; *P*=0.056, Log rank (Mantel–Cox) test. Blue indicates low PKCζ expression level, green medium, and beige high.

After relieving its auto-inhibition, active PKCζ kinase phosphorylates downstream substrates (Standaert et al., 1999; Yamanaka et al., 2001), and a number of its substrates have been identified. Par3 is one substrate, but it is not clear that Par3 phosphorylation is required in order to trigger epithelial cell polarisation (Hirose et al., 2002; Nagai-Tamai et al., 2002). We saw no change in Par3 protein levels or in gel mobility after PKCζ inhibition. Mammalian Lgl, an established member of the Scribble polarisation complex, has also been characterised as a PKCζ substrate. Lgl binds to Par6 and to PKCζ, and its phosphorylation by PKCζ is important for polarisation of embryonic fibroblasts (Plant et al., 2003). However, we saw no changes in Lgl (or Par1) phosphorylation after PKCζ inhibition in these mammary acini.

The first PDZ domain of Par3 has been shown to interact with Par6 (Joberty et al., 2000), and Par3 can bind directly to PKCζ through its atypical PKC (aPKC) binding domain (Izumi et al., 1998). In agreement with these observations, we show that Par3 forms a complex with both Par6 and PKCζ in polarising primary epithelial cells. However, after JNK blockade, in which polarisation had failed, Par3 still had the ability to bind to Par6 but its interaction with PKCζ was lost. This suggests that in the unpolarised MECs, a preformed complex of Par3 and Par6 exists, but that PKCζ is phosphorylated at T410 and activated only when the cells begin to establish polarity, and then forms part of the complex. By contrast, it has been shown that a Par3/Par6/aPKC cassette is present in unpolarised and fully polarised MDCK cells (Yamanaka et al., 2001), therefore complex formation might differ between model systems. We also see that phospho-PKCζ forms a complex with active Cdc42 early in acinus development. Upon JNK blockade, the levels of both proteins are reduced, but the two proteins still interact, suggesting that this part of the Par complex can form before cells fully polarise.

More interestingly, overexpression of a kinase-dead PKCζ mutant induced a more dramatic phenotype, i.e. the formation of incompletely polarised multi-acinar structures, with early hyperproliferation and defective lumen clearance. This PKCζ mutant cannot be activated either by phosphorylation at T410, or by T410-independent means. Early during acinus formation (D4) the structures infected with kinase-dead PKCζ displayed hyperproliferation, which we deem responsible for the eventual generation of the multi-acinar structures. In a range of studies in MCF10A acini, overexpression of oncogenes led to hyperproliferation and the formation of such structures (Bundy et al., 2005; Irie et al., 2005; Isakoff et al., 2005; Mohankumar et al., 2008; Seton-Rogers et al., 2004). In addition, activation of overexpressed ErbB2 was found to re-initiate proliferation in MCF10A acini, leading to the formation of multi-acinar structures with filled lumena (Muthuswamy et al., 2001).

Our data suggests that PKCζ kinase activity plays two roles (not necessarily independent but separable) during acinus formation: (1) facilitation of cell polarisation by a mechanism requiring regulation of kinase activity through phosphorylation at T410; and (2) suppression of cell proliferation early in the morphogenetic process to necessarily facilitate establishment of cell polarisation, cell–cell adhesion and, finally, lumen clearance. Failure of the latter function allows what looks like potent early lumenal cell proliferation, with the generation of a resultant large mass of lumenal cells. This overpowers the capacity of the ECM-supported cell polarisation machinery and the formation and maintenance of cell–cell junctions, resulting in the formation of the large structures resembling fused acini. However, we would suggest that they are not formed by fusion but arise from failure (or multiple failures) of the ECM-supported outer cells to establish or maintain comprehensive cell–cell adhesions. Noteworthy is the fact that by D10, when normal acini have all but cleared their lumena, these structures still have filled lumena but show low levels of proliferation and phospho-ERK (Fig. 7E). Thus, increased lumenal cell survival capacity might also be a feature of the phenotype. The simplest mechanism that we can propose is that epithelial cells undergoing acinus formation require a phosphorylation-independent basal/general PKCζ activity that supports proliferation restriction and a phosphorylation-induced, probably compartmentalized, PKCζ activity that supports cell polarisation.

We note that the fraction of PKCζ that distributes to the sites of tight junction assembly in developing primary acini and complexes with the Par proteins is phosphorylated on T410 in its kinase domain and differs in its distribution from the unphosphorylated pool (which does not colocalise with ZO-1) (supplementary material Figs S1 and S3). This supports our concept of the presence of two functionally separate pools of PKCζ. Such a separation of the populations of ‘activated’ phospho-T410-PKCζ and ‘non-phospho-activated’ PKCζ has also recently been observed in epithelium within the epidermis in vivo (Tunggal et al., 2005).

There is a certain level of correlation with the distribution of phospho-PKCζ in the developing mammary gland, in vivo. Increased expression of phospho-PKCζ parallels epithelisation of the gland at puberty and it co-distributes with ZO-1, suggesting a role in establishing cell polarity. Phospho-PKCζ levels also increase in the transition from late pregnancy to lactation, and it is lost in involution. In pregnancy and lactation, phospho-PKCζ distributes to the apical region of the alveolar epithelial cells, but it does not co-distribute with ZO1. Thus, in the maturing and mature secretary gland it might play a new role, perhaps secretion-related.

This impact on cell proliferation is highly reminiscent of the actions of a tumour suppressor and we therefore found it of interest to analyse PKCζ expression in breast cancer. In a screen of microarray data from 295 breast cancer patients (van de Vijver et al., 2002), we found that low and high levels of PKCζ mRNA expression correlated with a shorter time to overall survival, with low expression levels being the more significant. Also, we found that in poorly differentiated tumours, low PKCζ transcript levels again correlated with a poor outcome. These analyses support the hypothesis that either high or low levels, but especially low levels of PKCζ activity, will result in cell proliferation and polarisation defects and promote tumour progression.

In summary, we demonstrate that PKCζ activity is necessary for the establishment of MEC polarity and for cell proliferation restriction during acinus formation. Phosphorylation of PKCζ at T410 seems crucial for its function within the 'polarising' Par complex. A functionally distinct, (T410 phosphorylation-independent) PKCζ activity regulates cell proliferation during acinus formation. In breast cancer, low levels of PKCζ mRNA are associated with a poor outcome for patients, again reflecting the importance of this activity to the organisation of the mammary epithelium and its potential protective capacity in disease.

Materials and Methods

Cell culture

Mouse mammary cells were harvested from mid-pregnant CD-1 mice as described previously (Murtagh et al., 2004). Cells were seeded on four-well chamber slides or on 6-cm tissue culture dishes coated with concentrated, growth-factor-depleted mouse tumour ECM (EHS-ECM; Matrigel, BD Biosciences). Cells were cultured for 4–48 hours with 5 ng/ml EGF (Promega), 5 μg/ml insulin, 1 μg/ml hydrocortisone and 50 μg/ml gentamycin (Sigma) in F12 medium (Life Technologies, Carlsbad, CA). MCF10A cells were cultured exactly as outlined previously (Debnath et al., 2003). Inhibitors used were myristoylated PKCζ psuedosubstrate inhibitor (10 μM), SP600125 (20 μM MCF10A or 50 μM primary cells) (Calbiochem). Inhibitors were added to primary cells at the time of plating, unless otherwise stated. Inhibitors were added on day 3 to MCF10A cells, and cells were harvested and fixed on D4 and D8, or D10 for virus experiments.

Antibodies

Antibodies used were anti-PKCζ and phospho-T410-PKCζ, phospho-EGFR, phospho-AKT, AKT, E-cadherin (Cell Signaling Technology); Par3, Scrib, phospho-42/44ERK, ERK, cleaved-caspase 3, cyclin D1 (Upstate Technology); Par6, phospho-p21, p21, p27, PKCζ (Santa Cruz Biotechnology); F-actin, FLAG M2, DM1A, GFP (Sigma); Cdc42 (Pierce); Gm130, β-catenin (BD Clontech); Rhodamine, phalloidin (Molecular Probes); Ki67 (Chemicon); ZO-1 (Zymed and Novus); and EGFR (Novus Biologicals).

Western blotting and immunoprecipitation

Whole-cell extracts were prepared in RIPA buffer (50 mM Tris-HCl pH 7.4, 1% NP40, 150 mM NaCl, 1 mM EDTA pH 8.0, 1 mM Na_3VO_4, 1 mM NaF) with protease inhibitor cocktail (Sigma). Samples were separated by gel electrophoresis (Bio-Rad) and transferred to Whatman nitrocellulose membranes for western blot analysis. For immunoprecipitations, supernatants were incubated with 2 μl of anti-Par3, anti-Par6 or anti-PKCζ antibody, and 45 μl of protein A bead suspension (Sigma). Samples were incubated at 4°C overnight with rotation. The immune complex was washed four times with lysis buffer. 2× Laemmli buffer was added and samples were boiled before loading onto 8–12% SDS PAGE gels. Cdc42 activation assay kit (Pierce) containing Pak1 PBD was used to bind and precipitate GTP-bound Cdc42 from 1 mg of total protein as per the manufacturer's instructions.

Kinase activity assay

PKCζ activity was measured using a kinase assay kit and a specific substrate for PKCζ (Upstate) and carried out according to the manufacturer's recommendations. The assay is based on phosphorylation of the specific substrate peptide using the transfer of the γ-phosphate of adenosine-5′-[^{32}P]triphosphate ([γ-^{32}P]ATP) by PKCζ. The phosphorylated substrate is then separated from the residual [γ-^{32}P]ATP using P81 phosphocellulose paper. Whole-cell lysates from three 6-cm plates were pooled and the immunoprecipitation was carried out as above with anti-PKCζ (Santa Cruz Biotechnology).

Lentivirus production

Genes (cDNAs) to be expressed were purchased from Addgene (catalogue numbers 10799, 10801, 10804, 10800 and 12254) and cloned from pCMV5, into pWPI. Enzymes were purchased from New England Biolabs and Roche (Quick Cloning kit). Cloned constructs were verified by PCR, digestion and sequencing (MWG, UK). Lentivector particles were generated by co-expressing the virion packaging and envelope elements (pCMV and pMD2G) and the vector genome in a producer cell (HEKs) using a calcium phosphate transfection kit (Invitrogen). Virus-containing medium was filtered through a 0.45 μm membrane and stored at –80°C. Viral samples were thawed at 37°C and spun at 13,000 ***g*** for 2 minutes before quantitation and addition to cells with 6 μg/ml of polybrene. Quicktitre Lentivirus Quantitation kit (Cell Biolabs) was used to quantitate virus particles per ml (VP/ml). Addition of 2.5×10^9 VP or ~250 μL of virus solution per well was sufficient for ~100% infection without toxicity.

MTT assay

Infected MCF10A cells were plated in a 96-well dish (six replicates per sample). On days 1–5, 50 μL of MTT (5 mg/ml in PBS) (Sigma) was added to each well and left for 3.5 hours at 37°C in darkness. MTT-containing medium was removed, and 200 μL of DMSO (Sigma) was added. Plates were analysed using a Wallac plate reader at an absorbance of 570 nm. The graph (generated in Excel) shown in Fig. 6C is for four independent experiments. A Student's *t*-test was used to assess differences in the slopes of the fitted lines.

Microscopy

Acini were fixed using 2% (MCF10A) or 4% (primary cells) paraformaldehyde for 20 minutes at room temperature. Cells were permeabilised using 0.5% Triton X-100 for 10 minutes at 4°C prior to blocking. Cells were incubated with primary antibodies overnight at 4°C in a humidity chamber and then with FITC, Texas-Red-conjugated, or Alexa Fluor 555 goat anti-mouse or anti-rabbit (Molecular Probes) secondary antibodies in darkness for 1 hour. Slides were mounted in Prolong Gold anti-fade reagent with DAPI (Molecular Probes). Images were captured using a Bio-Rad MRC 1024 or a Carl Zeiss Laser Scanning LSM 510 (Version 3.2 SP2) Meta Confocal microscope.

Immunofluorescence on mouse mammary tissue sections

Double-immunofluorescence labelling was performed on sections cut from PBS-buffered formalin-fixed and paraffin-embedded inguinal mammary glands. In brief, after de-waxing in xylene, antigen retrieval was performed using 1 mM EDTA, pH 9.0 in a pressure cooker. The sections were blocked for 30 minutes in Image-iT FX Signal Enhancer solution (Invitrogen) followed by 15 minutes of 2.5% horse serum (Invitrogen), both at room temperature (RT). Anti-phospho-PKCζ antibody was incubated for 30 minutes at RT, whereas anti-PKCζ was incubated overnight at 4°C, each followed by incubation with rat anti-ZO-1 antibody. Alexa Fluor 488-labelled goat-anti-rabbit (green) (dilution 1:1000) and Alexa Fluor 594-labelled goat anti-rat (red) antibodies (Invitrogen) were incubated for 20 minutes at RT. For negative controls, no primary antibodies were used. Slides were mounted using ProLong Gold antifade with DAPI (Invitrogen). Images were obtained using an F-view digital camera attached to an inverted Olympus IX-51 fluorescence microscope. Images were analysed using Cell-P software (Olympus, UK).

Microarray analysis

Relevant histopathological and clinical data relating to 295 patients with breast cancer (van de Vijver et al., 2002) was downloaded from a publicly available website (Rosetta Inpharmatics; http://www.rii.com). For gene analysis, the log ratios of gene expression values were used without modification. Tumour samples were classified by first separating into quartiles according to mRNA expression and then, because trends within the data were complex, three groups were used for the final analysis. PKCζ expression distribution was binned into three groups: low (74 patients), medium (143 patients) and high (73 patients) expression, with 295 patients total. SPSS 15 software (SPSS, Chicago, IL) was used to analyse array data. Kaplan–Meier analysis was performed to compare time-to-event and PKCζ expression level of the three groups using the Log-Rank (Mantel–Cox) test.

Data

All western blot, immunoprecipitation, kinase and microscopy analyses were carried out at least three times on independent cell preparations. Images shown are representative of these multiple analyses.

We are grateful for funding from Science Foundation Ireland and the Health Research Board (Ireland). Torstein Stein is supported by a Breakthrough Breast Cancer (UK) project grant. We acknowledge John Kennedy and Roderick Ferrier for their technical work on the immunofluorescence of mouse mammary tissue sections.

Supplementary material available online at
http://jcs.biologists.org/cgi/content/full/123/19/3316/DC1

References

Aranda, V., Haire, T., Nolan, M. E., Calarco, J. P., Rosenberg, A. Z., Fawcett, J. P., Pawson, T. and Muthuswamy, S. K. (2006). Par6-aPKC uncouples ErbB2 induced disruption of polarized epithelial organization from proliferation control. *Nat. Cell Biol.* **8**, 1235-1245.

Aranda, V., Nolan, M. E. and Muthuswamy, S. K. (2008). Par complex in cancer: a regulator of normal cell polarity joins the dark side. *Oncogene* **27**, 6878-6887.

Baranwal, S. and Alahari, S. K. (2009). Molecular mechanisms controlling E-cadherin expression in breast cancer. *Biochem. Biophys. Res. Commun.* **384**, 6-11.

Barcellos-Hoff, M. H., Aggeler, J., Ram, T. G. and Bissell, M. J. (1989). Functional differentiation and alveolar morphogenesis of primary mammary cultures on reconstituted basement membrane. *Development* **105**, 223-235.

Bilder, D., Schober, M. and Perrimon, N. (2003). Integrated activity of PDZ protein complexes regulates epithelial polarity. *Nat. Cell Biol.* **5**, 53-58.

Blatchford, D. R., Hendry, K. A., Turner, M. D., Burgoyne, R. D. and Wilde, C. J. (1995). Vectorial secretion by constitutive and regulated secretory pathways in mammary epithelial cells. *Epithelial Cell Biol.* **4**, 8-16.

Blatchford, D. R., Quarrie, L. H., Tonner, E., McCarthy, C., Flint, D. J. and Wilde, C. J. (1999). Influence of microenvironment on mammary epithelial cell survival in primary culture. *J. Cell Physiol.* **181**, 304-311.

Brembeck, F. H., Rosario, M. and Birchmeier, W. (2006). Balancing cell adhesion and Wnt signaling, the key role of beta-catenin. *Curr. Opin. Genet. Dev.* **16**, 51-59.

Bundy, L., Wells, S. and Sealy, L. (2005). C/EBPbeta-2 confers EGF-independent growth and disrupts the normal acinar architecture of human mammary epithelial cells. *Mol. Cancer* **4**, 43.

Capaldo, C. T. and Macara, I. G. (2007). Depletion of E-cadherin disrupts establishment but not maintenance of cell junctions in Madin-Darby canine kidney epithelial cells. *Mol. Biol. Cell* **18**, 189-200.

Cenni, V., Doppler, H., Sonnenburg, E. D., Maraldi, N., Newton, A. C. and Toker, A. (2002). Regulation of novel protein kinase C epsilon by phosphorylation. *Biochem. J.* **363**, 537-545.

Chou, M. M., Hou, W., Johnson, J., Graham, L. K., Lee, M. H., Chen, C. S., Newton, A. C., Schaffhausen, B. S. and Toker, A. (1998). Regulation of protein kinase C zeta by PI 3-kinase and PDK-1. *Curr. Biol.* **8**, 1069-1077.

Debnath, J. and Brugge, J. S. (2005). Modelling glandular epithelial cancers in three-dimensional cultures. *Nat. Rev. Cancer* **5**, 675-688.

Debnath, J., Mills, K. R., Collins, N. L., Reginato, M. J., Muthuswamy, S. K. and Brugge, J. S. (2002). The role of apoptosis in creating and maintaining luminal space within normal and oncogene-expressing mammary acini. *Cell* **111**, 29-40.

Debnath, J., Muthuswamy, S. K. and Brugge, J. S. (2003). Morphogenesis and oncogenesis of MCF-10A mammary epithelial acini grown in three-dimensional basement membrane cultures. *Methods* **30**, 256-268.

Etienne-Manneville, S. and Hall, A. (2001). Integrin-mediated activation of Cdc42 controls cell polarity in migrating astrocytes through PKCzeta. *Cell* **106**, 489-498.

Fukata, M., Nakagawa, M., Itoh, N., Kawajiri, A., Yamaga, M., Kuroda, S. and Kaibuchi, K. (2001a). Involvement of IQGAP1, an effector of Rac1 and Cdc42 GTPases, in cell-cell dissociation during cell scattering. *Mol. Cell. Biol.* **21**, 2165-2183.

Fukata, Y., Amano, M. and Kaibuchi, K. (2001b). Rho-Rho-kinase pathway in smooth muscle contraction and cytoskeletal reorganization of non-muscle cells. *Trends Pharmacol. Sci.* **22**, 32-39.

Galvez, A. S., Duran, A., Linares, J. F., Pathrose, P., Castilla, E. A., Abu-Baker, S., Leitges, M., Diaz-Meco, M. T. and Moscat, J. (2009). Protein kinase Czeta represses the interleukin-6 promoter and impairs tumorigenesis in vivo. *Mol. Cell. Biol.* **29**, 104-115.

Goldstein, B. and Macara, I. G. (2007). The PAR proteins: fundamental players in animal cell polarization. *Dev. Cell* **13**, 609-622.

Gotta, M., Abraham, M. C. and Ahringer, J. (2001). CDC-42 controls early cell polarity and spindle orientation in C. elegans. *Curr. Biol.* **11**, 482-488.

Gschwendt, M., Kittstein, W. and Marks, F. (1991). Protein kinase C activation by phorbol esters: do cysteine-rich regions and pseudosubstrate motifs play a role? *Trends Biochem. Sci.* **16**, 167-169.

Hirai, T. and Chida, K. (2003). Protein kinase Czeta (PKCzeta): activation mechanisms and cellular functions. *J. Biochem.* **133**, 1-7.

Hirohashi, S. and Kanai, Y. (2003). Cell adhesion system and human cancer morphogenesis. *Cancer Sci.* **94**, 575-581.

Hirose, T., Izumi, Y., Nagashima, Y., Tamai-Nagai, Y., Kurihara, H., Sakai, T., Suzuki, Y., Yamanaka, T., Suzuki, A., Mizuno, K. et al. (2002). Involvement of ASIP/PAR-3 in the promotion of epithelial tight junction formation. *J. Cell Sci.* **115**, 2485-2495.

Irie, H. Y., Pearline, R. V., Grueneberg, D., Hsia, M., Ravichandran, P., Kothari, N., Natesan, S. and Brugge, J. S. (2005). Distinct roles of Akt1 and Akt2 in regulating cell migration and epithelial-mesenchymal transition. *J. Cell Biol.* **171**, 1023-1034.

Isakoff, S. J., Engelman, J. A., Irie, H. Y., Luo, J., Brachmann, S. M., Pearline, R. V., Cantley, L. C. and Brugge, J. S. (2005). Breast cancer-associated PIK3CA mutations are oncogenic in mammary epithelial cells. *Cancer Res.* **65**, 10992-11000.

Izumi, Y., Hirose, T., Tamai, Y., Hirai, S., Nagashima, Y., Fujimoto, T., Tabuse, Y., Kemphues, K. J. and Ohno, S. (1998). An atypical PKC directly associates and colocalizes at the epithelial tight junction with ASIP, a mammalian homologue of Caenorhabditis elegans polarity protein PAR-3. *J. Cell Biol.* **143**, 95-106.

Joberty, G., Petersen, C., Gao, L. and Macara, I. G. (2000). The cell-polarity protein Par6 links Par3 and atypical protein kinase C to Cdc42. *Nat. Cell Biol.* **2**, 531-539.

Kass, L., Erler, J. T., Dembo, M. and Weaver, V. M. (2007). Mammary epithelial cell: influence of extracellular matrix composition and organization during development and tumorigenesis. *Int. J. Biochem. Cell Biol.* **39**, 1987-1994.

Kemphues, K. (2000). PARsing embryonic polarity. *Cell* **101**, 345-348.

Kemphues, K. J., Priess, J. R., Morton, D. G. and Cheng, N. S. (1988). Identification of genes required for cytoplasmic localization in early C. elegans embryos. *Cell* **52**, 311-320.

Keranen, L. M., Dutil, E. M. and Newton, A. C. (1995). Protein kinase C is regulated in vivo by three functionally distinct phosphorylations. *Curr. Biol.* **5**, 1394-1403.

Lin, D., Edwards, A. S., Fawcett, J. P., Mbamalu, G., Scott, J. D. and Pawson, T. (2000). A mammalian PAR-3-PAR-6 complex implicated in Cdc42/Rac1 and aPKC signalling and cell polarity. *Nat. Cell Biol.* **2**, 540-547.

Macara, I. G. (2004). Par proteins: partners in polarization. *Curr. Biol.* **14**, R160-R162.

Margolis, B. and Borg, J. P. (2005). Apicobasal polarity complexes. *J. Cell Sci.* **118**, 5157-5159.

Mohankumar, K. M., Perry, J. K., Kannan, N., Kohno, K., Gluckman, P. D., Emerald, B. S. and Lobie, P. E. (2008). Transcriptional activation of signal transducer and activator of transcription (STAT) 3 and STAT5B partially mediate homeobox A1-stimulated oncogenic transformation of the immortalized human mammary epithelial cell. *Endocrinology* **149**, 2219-2229.

Murtagh, J., McArdle, E., Gilligan, E., Thornton, L., Furlong, F. and Martin, F. (2004). Organization of mammary epithelial cells into 3D acinar structures requires glucocorticoid and JNK signaling. *J. Cell Biol.* **166**, 133-143.

Muthuswamy, S. K., Li, D., Lelievre, S., Bissell, M. J. and Brugge, J. S. (2001). ErbB2, but not ErbB1, reinitiates proliferation and induces luminal repopulation in epithelial acini. *Nat. Cell Biol.* **3**, 785-792.

Nagai-Tamai, Y., Mizuno, K., Hirose, T., Suzuki, A. and Ohno, S. (2002). Regulated protein-protein interaction between aPKC and PAR-3 plays an essential role in the polarization of epithelial cells. *Genes Cells* **7**, 1161-1171.

Nguyen, D. A. and Neville, M. C. (1998). Tight junction regulation in the mammary gland. *J. Mammary Gland Biol. Neoplasia* **3**, 233-246.

Nolan, M. E., Aranda, V., Lee, S., Lakshmi, B., Basu, S., Allred, D. C. and Muthuswamy, S. K. (2008). The polarity protein Par6 induces cell proliferation and is overexpressed in breast cancer. *Cancer Res.* **68**, 8201-8209.

Petersen, O. W., Ronnov-Jessen, L., Howlett, A. R. and Bissell, M. J. (1992). Interaction with basement membrane serves to rapidly distinguish growth and differentiation pattern of normal and malignant human breast epithelial cells. *Proc. Natl. Acad. Sci. USA* **89**, 9064-9068.

Plant, P. J., Fawcett, J. P., Lin, D. C., Holdorf, A. D., Binns, K., Kulkarni, S. and Pawson, T. (2003). A polarity complex of mPar-6 and atypical PKC binds, phosphorylates and regulates mammalian Lgl. *Nat. Cell Biol.* **5**, 301-308.

Qiu, R. G., Abo, A. and Steven Martin, G. (2000). A human homolog of the C. elegans polarity determinant Par-6 links Rac and Cdc42 to PKCzeta signaling and cell transformation. *Curr. Biol.* **10**, 697-707.

Reginato, M. J., Mills, K. R., Becker, E. B., Lynch, D. K., Bonni, A., Muthuswamy, S. K. and Brugge, J. S. (2005). Bim regulation of lumen formation in cultured mammary epithelial acini is targeted by oncogenes. *Mol. Cell. Biol.* **25**, 4591-4601.

Sequeira, S. J., Ranganathan, A. C., Adam, A. P., Iglesias, B. V., Farias, E. F. and Aguirre-Ghiso, J. A. (2007). Inhibition of proliferation by PERK regulates mammary acinar morphogenesis and tumor formation. *PLoS ONE* **2**, e615.

Seton-Rogers, S. E., Lu, Y., Hines, L. M., Koundinya, M., LaBaer, J., Muthuswamy, S. K. and Brugge, J. S. (2004). Cooperation of the ErbB2 receptor and transforming growth factor beta in induction of migration and invasion in mammary epithelial cells. *Proc. Natl. Acad. Sci. USA* **101**, 1257-1262.

Shin, K., Fogg, V. C. and Margolis, B. (2006). Tight junctions and cell polarity. *Annu. Rev. Cell Dev. Biol.* **22**, 207-235.

Standaert, M. L., Galloway, L., Karnam, P., Bandyopadhyay, G., Moscat, J. and Farese, R. V. (1997). Protein kinase C-zeta as a downstream effector of phosphatidylinositol 3-kinase during insulin stimulation in rat adipocytes. Potential role in glucose transport. *J. Biol. Chem.* **272**, 30075-30082.

Standaert, M. L., Bandyopadhyay, G., Perez, L., Price, D., Galloway, L., Poklepovic, A., Sajan, M. P., Cenni, V., Sirri, A., Moscat, J. et al. (1999). Insulin activates protein kinases C-zeta and C-lambda by an autophosphorylation-dependent mechanism and stimulates their translocation to GLUT4 vesicles and other membrane fractions in rat adipocytes. *J. Biol. Chem.* **274**, 25308-25316.

Suzuki, A., Yamanaka, T., Hirose, T., Manabe, N., Mizuno, K., Shimizu, M., Akimoto, K., Izumi, Y., Ohnishi, T. and Ohno, S. (2001). Atypical protein kinase C is involved in the evolutionarily conserved par protein complex and plays a critical role in establishing epithelia-specific junctional structures. *J. Cell Biol.* **152**, 1183-1196.

Tsutakawa, S. E., Medzihradszky, K. F., Flint, A. J., Burlingame, A. L. and Koshland, D. E., Jr (1995). Determination of in vivo phosphorylation sites in protein kinase C. *J. Biol. Chem.* **270**, 26807-26812.

Tunggal, J. A., Helfrich, I., Schmitz, A., Schwarz, H., Gunzel, D., Fromm, M., Kemler, R., Krieg, T. and Niessen, C. M. (2005). E-cadherin is essential for in vivo epidermal barrier function by regulating tight junctions. *EMBO J.* **24**, 1146-1156.

van de Vijver, M. J., He, Y. D., van't Veer, L. J., Dai, H., Hart, A. A., Voskuil, D. W., Schreiber, G. J., Peterse, J. L., Roberts, C., Marton, M. J. et al. (2002). A gene-expression signature as a predictor of survival in breast cancer. *N. Engl. J. Med.* **347**, 1999-2009.

Weaver, V. M., Petersen, O. W., Wang, F., Larabell, C. A., Briand, P., Damsky, C. and Bissell, M. J. (1997). Reversion of the malignant phenotype of human breast cells in three-dimensional culture and in vivo by integrin blocking antibodies. *J. Cell Biol.* **137**, 231-245.

Weaver, V. M., Lelievre, S., Lakins, J. N., Chrenek, M. A., Jones, J. C., Giancotti, F., Werb, Z. and Bissell, M. J. (2002). beta4 integrin-dependent formation of polarized three-dimensional architecture confers resistance to apoptosis in normal and malignant mammary epithelium. *Cancer Cell* **2**, 205-216.

Wodarz, A. (2000). Tumor suppressors: linking cell polarity and growth control. *Curr. Biol.* **10**, R624-R626.

Wodarz, A. and Nathke, I. (2007). Cell polarity in development and cancer. *Nat. Cell Biol.* **9**, 1016-1024.

Yamanaka, T., Horikoshi, Y., Suzuki, A., Sugiyama, Y., Kitamura, K., Maniwa, R., Nagai, Y., Yamashita, A., Hirose, T., Ishikawa, H. et al. (2001). PAR-6 regulates aPKC activity in a novel way and mediates cell-cell contact-induced formation of the epithelial junctional complex. *Genes Cells* **6**, 721-731.

Zhan, L., Rosenberg, A., Bergami, K. C., Yu, M., Xuan, Z., Jaffe, A. B., Allred, C. and Muthuswamy, S. K. (2008). Deregulation of scribble promotes mammary tumorigenesis and reveals a role for cell polarity in carcinoma. *Cell* **135**, 865-878.